**Research Article** **Open Access**

Sharon Kehoe*, Salma Amensag, Mark Looney, Robert J. Abraham, and Daniel Boyd*

# "Imageable" Zinc-Silicate Glass Microspheres For Transarterial Embolization: A Renal Artery Embolization Study.

DOI 10.1515/bglass-2015-0007
Received Jun 08, 2015; accepted Jun 08, 2015

**Abstract:** Intrinsically radiopaque (imageable) microspheres for transarterial embolization (TAE) are required to enable real-time intraprocedural feedback and definition of spatial distribution patterns of embolic materials in target tissues. This pilot study evaluates acute and sub-chronic safety and efficacy of imageable zinc-silicate (Zn-Si) glass microspheres in a swine renal artery embolization (RAE) model. Eight swine were divided into two cohorts. Clinical determinants of embolization effectiveness, including imageability, deliverability and temporal/spatial distribution of microspheres in target tissues were assessed. Subsequently, cohort I and II were used to evaluate the acute and subchronic host response against the Zn-Si microspheres versus a clinical control. The developed microspheres provide for direct intraprocedural feedback using standard diagnostic imaging techniques. Fluoroscopy correlated with *ex-vivo* high-resolution radiography, CT and micro-CT, demonstrating high imageability, excellent spatial distribution and packing of the Zn-Si microspheres. At follow-up, infarction of the embolized kidneys was noted without any major adverse tissue reaction. Mild recanalization was observed microscopically for both experimental and control microspheres. Zn-Si microspheres permit the definition of spatial distribution in a target tissue, consequently permitting the optimization, personalization and improvement of TAE techniques.

**Keywords:** Zinc-Silicate Glass; Embolic Microspheres; Radiopacity; Embolization; Swine Renal Artery Embolization; Biocompatibility

## 1 Introduction

The broad compositional palette of bioactive glasses provides for a range of physico-chemical and mechanical properties contiguous with tailored biological responses in a range of applications within orthopedic and dental applications, and beyond [1]. Transarterial embolization (TAE) with microspheres is as an effective technique in the treatment of arteriovenous malformations and hypervascularized tumors (including uterine fibroid and prostate arterial embolization) [2, 3]. Conventional embolic biomaterials are primarily based on polyvinyl-alcohol (PVA) or trisacryl gelatin (TAG). These devices are radiolucent and require blending with contrast media, prior to their delivery, such that the contrast media can act as a surrogate measure of the temporal and spatial distribution of microspheres within the target tissue. As has been pointed out by Sharma *et al.* [4], the inability to directly monitor embolic microspheres "preclude[s] ideal spatial delivery" and does not permit accurate assessment of their terminal locations. It has been further pointed [4–6], that the provision of an intrinsically radiopaque embolic microsphere

***Corresponding Author: Sharon Kehoe:** ABK Biomedical Inc. 1344 Summer Street, Suite 212, Halifax, B3H0A8; Department of Applied Oral Sciences, Dalhousie University, PO Box 15000, Halifax, NS, Canada, B3H 4R2; E-mail: s.kehoe@abkbiomedical.com/d.boyd@abkbiomedical.com; Tel.: (902)-442-4009; Address: ABK Biomedical Inc., Halifax, NS, B3H 0A8, Canada.

**Salma Amensag:** ABK Biomedical Inc. 1344 Summer Street, Suite 212, Halifax, B3H0A8.

**Mark Looney:** ABK Biomedical Inc. 1344 Summer Street, Suite 212, Halifax, B3H0A8.

**Robert J. Abraham:** ABK Biomedical Inc. 1344 Summer Street, Suite 212, Halifax, B3H0A8; School of Biomedical Engineering, Dalhousie University, PO Box 15000, Halifax, NS, Canada, B3H 4R2; Department of Diagnostic Imaging and Interventional Radiology, QE II Health Sciences Centre, Halifax, NS, Canada, B3H 3A7.

***Corresponding Author: Daniel Boyd:** ABK Biomedical Inc. 1344 Summer Street, Suite 212, Halifax, B3H0A8; Department of Applied Oral Sciences, Dalhousie University, PO Box 15000, Halifax, NS, Canada, B3H 4R2; School of Biomedical Engineering, Dalhousie University, PO Box 15000, Halifax, NS, Canada, B3H 4R2; Department of Diagnostic Imaging and Interventional Radiology, QE II Health Sciences Centre, Halifax, NS, Canada, B3H 3A7; E-mail: s.kehoe@abkbiomedical.com/d.boyd@abkbiomedical.com; Tel.: (902)-442-4009; Address: ABK Biomedical Inc., Halifax, NS, B3H 0A8, Canada.

for TAE would (a) define true spatial distribution of embolic materials in a target tissue, (b) provide real-time intraprocedural feedback, (c) optimize, personalize and improve TAE techniques, and as a consequence, (d) standardize material choice and procedural technique with a high degree of confidence.

PVA and TAG materials have been shown to provide a combination of biological (including thrombus formation, cell adhesion, and inflammation) and mechanical mechanisms of occlusion [7–9]. Conventional embolic biomaterials have relatively high compressibility, a property which is thought to permit ease of deliverability through micro-catheters (where internal diameters are on the order of c. 700 $\mu$m). For example, Embosphere® microspheres can tolerate compressibility up to 30% without undergoing any fragmentation, but can swell upon mixing with contrast media to result in a 10-40% increase in diameter [10]. Excessive compressibility can lead to deformation of the embolic agent in-situ and can increase the potential for embolic instability – arising from the subsequent redistribution of microspheres and revascularization of targeted tissue [3].

To overcome these limitations, we recently reported the development of a multicomponent 0.562 $SiO_2$–0.035 CaO–0.188 ZnO–0.068 $La_3O_2$–0.042 $TiO_2$–0.035 MgO–0.035 SrO–0.035 $Na_2O$ glass microsphere for embolization procedures that would permit direct intraprocedural feedback while limiting the use of contrast media. This glass was designed as an inherently radiopaque, cytocompatible and non-compressible microsphere for embolization therapies such as treatment of arteriovenous malformations and hypervascularized tumors [11–13]. Initial benchtop CT evaluations of the zinc-silicate (Zn-Si) glass demonstrated high radiopacity (c. 8,000HU) versus conventional 50% contrast media (c. 2,400HU). Subsequent to these studies, significant research has been published with respect to composition-structure-property relationships of these materials as a function of spheroidization, effects of single and double dose gamma irradiation (30-60 kGy) and accelerated aging (up to 24 months) [14–16]. In addition, and given the propensity for glass biomaterials to release constituent metal cations under physiological conditions, the ion release characteristics and genotoxic potential for these materials has also been clarified in the literature [17]. To date, the material demonstrates excellent melt characteristics, spheroidization capacity, cytocompatibility, radiopacity and genotoxicity.

The purpose of this work is to assess, in a pilot study and for the first time, Zn-Si microspheres for: (i) their spatial and temporal distribution in renal vasculature during routine intraprocedural fluoroscopy and (ii) their embolization effectiveness and associated host response markers in acute and sub-chronic studies. The first stage of this study comprised a screening step, whereby an acute evaluation of the imaging, ease of deliverability and embolization effectiveness for Zn–Si microspheres (40-150 $\mu$m, 150-300 $\mu$m and 300-500 $\mu$m) in a swine renal artery embolization (RAE) model were assessed [4, 5, 7, 8]. In the second stage of this study, unilateral RAE were performed using 40-150 $\mu$m Zn–Si microspheres *(40-150 $\mu$m microspheres being deemed to represent the worst-case scenario in terms of host response due to their high surface to volume ratio)* to evaluate embolization effectiveness, temporal and spatial distribution and biological response 29 days post-embolization. Macroscopic, pathologic and histologic evaluations of the inflammatory reactions were performed to evaluate overall safety and efficacy for Zn–Si microspheres in comparison to a commercial embolic microsphere.

# 2 Materials and Methods

## 2.1 Materials

Multi-component zinc silicate glass microspheres having the formulation: 0.562 $SiO_2$–0.035 CaO–0.188 ZnO–0.068 $La_3O_2$–0.042 $TiO_2$–0.035 MgO–0.035 SrO–0.035 $Na_2O$ were evaluated in this study. Microspheres were synthesized as described previously [16, 17]: briefly, analytical grade reagents: silicon dioxide, calcium carbonate, zinc oxide, magnesium oxide, lanthanum (III) oxide, strontium carbonate, titanium dioxide and sodium carbonate were weighed and homogeneously blended for 1 h. Each lot of powder was placed in 2 platinum crucibles (500 cc each), fired (1350°C, 1 h) using an electric furnace and shock quenched into distilled water. The resulting glass frit was dried in an oven (100°C, overnight), ground with a BICO plate grinder (alumina plates) and sieved to retrieve particles in the clinically relevant size ranges of 40-150 $\mu$m, 150-300 $\mu$m and 300-500 $\mu$m for embolization therapies. Glass particles were then subjected to flame spherodization using a propane oxygen flame to transform the morphology of the glass frit to a microsphere. Microspheres were packaged dry in clean containers and sterilized using 30 kGy gamma irradiation. The control article was the commercially available trisacryl gelatin microsphere - Embosphere®. Embosphere was supplied packaged wet (in saline) in 2.0 mL pre-filled vials (Merit Medical, Rockland, MD, USA).

**Table 1:** Zn–Si microsphere and Embosphere® allocation.

| Cohort/Animal No. | Treatment | Size Range | Embolization Procedure | No. of Embolizations |
|---|---|---|---|---|
| **Cohort I/Ac-01** | Zn–Si glass | 300-500 | Whole kidney embolization | n=1 |
| | Embosphere® | 300-500 | | n=1 |
| **Cohort I/Ac-02** | Zn–Si glass | 300-500 | Subsegmental renal artery | n=1 |
| | Embosphere® | 300-500 | (cranial/caudal pole) | n=1 |
| **Cohort I/Ac-03** | Zn-Si glass | 300-500 | Subsegmental renal artery | n=1 |
| | | 150-300 | (cranial/caudal pole) | n=1 |
| | | 40-150 | | n=2 |
| **Cohort II/** | Zn-Si glass | 40-150 | Subsegmental renal artery | n=3 |
| **Ac-04 to Ac-08** | Embosphere® | 40-120 | (cranial/caudal pole) | n=2 |

## 2.2 Swine RAE Procedures & Embolization Effectiveness.

This work received ethical approval from the Comite institutionnel de protection des animaux d'AccelLAB and were in compliance with the Canadian Council on Animal Care regulations (CCAC). All animals were housed under conditions consistent with all Provincial and National regulations and received standard medical care from animal health technicians.

8 animals (Identified as Ac-01 to Ac-08) were divided into 2 cohorts (Table 1) to examine (a) clinical determinants of embolization effectiveness, including temporal and spatial distribution of microspheres and radiopacity and (b) the acute and sub-chronic host response to both the Zn-Si microspheres and Embosphere®. In cohort I, three domestic pigs (sus scrofa species, Landrace-Yorkshire), weighing between 53 and 60 kg were randomly assigned for whole kidney or bilateral RAE, to clinically demonstrate ease of deliverability for each particle size distribution of the Zn-Si glass microsphere. In cohort II, five miniswine (sus scrofa species, Yucatan), weighting between 42 and 45 kg (9-11 months), received sub-segmental (cranial or caudal pole) embolization, using 40-150 $\mu$m sized Zn–Si microspheres. Equivalent sizes of a commercial control were used throughout (as per Table 1).

All animals were anesthetized with ketamine (Bimeda-MTC, Cambridge, Ontario, Canada), azaperone (Janssen Pharmaceutica, Beerse, Belgium) and atropine (Rafter, Calgary, Alberta, Canada) administered intramuscularly. Animals were placed in dorsal recumbency, and the inguinal region was shaved and disinfected prior to arterial access. Bupivacaine 0.25% (up to 5 mL/surgical site Hospira, Inc., Lake Forest, IL, USA) was infiltrated into the inguinal puncture site to achieve local anesthesia and ultrasound guidance, percutaneous femoral arterial access was achieved using a 4 Fr micropuncture access system (Cook Inc., Bloomington, IN). Under fluoroscopic guidance, a selective 4Fr Slipcath Cobra 2 diagnostic catheter (Cook Inc., Bloomington, IN) was advanced into the proximal renal artery. For embolization using 40-150 $\mu$m or 100-300 $\mu$m microspheres, a Renegade Hi-Flo microcatheter (Boston Scientific, Marlborough, MA) was advanced co-axially and positioned within the cranial or caudal intraparenchymal segmental renal artery branch. For embolization using 300-500 $\mu$m Zn–Si microspheres, the 4 Fr diagnostic catheter was selectively advanced into the intraparenchymal segmental renal artery branch over a 0.035" Terumo Glidewire (Terumo Corporation, Tokyo, Japan). Pre-embolization angiographic images (Siemens Fluoroscope, Hicor, Germany) of the vessel were obtained using 50% saline diluted contrast media (Omipaque, GE Healthcare). Zn–Si and control microspheres were injected into the selected artery under fluoroscopic guidance. For clarity, Embospheres® were delivered post dilution in 50% contrast media solution according to manufacturers instructions. Zn-Si microspheres were delivered using sterile saline in order to evaluate their fluoroscopic visibility during injection. Effective stasis, for both experimental and control microspheres, was deemed complete by injecting 50% contrast media into the targeted segmental artery and observing its stasis for 5 or more cardiac pulsations [18]. Post-embolization angiography was performed, with all arteries in the observation region qualitatively evaluated for arterial perforation or rupture and embolization effectiveness by an interventional radiologist (RJA). Following closure, the anesthetic agent was discontinued and the animals ventilated until the return of normal respiration.

Immediately post-embolization (cohort I and II) and 29 days post-embolization (cohort II), an interventional radiologist (RJA) blindly evaluated embolization effectiveness, durability of occlusion, and recanalization for each animal based on the following numerical grading scale [19]: 0=No angiographic visible signs of arte-

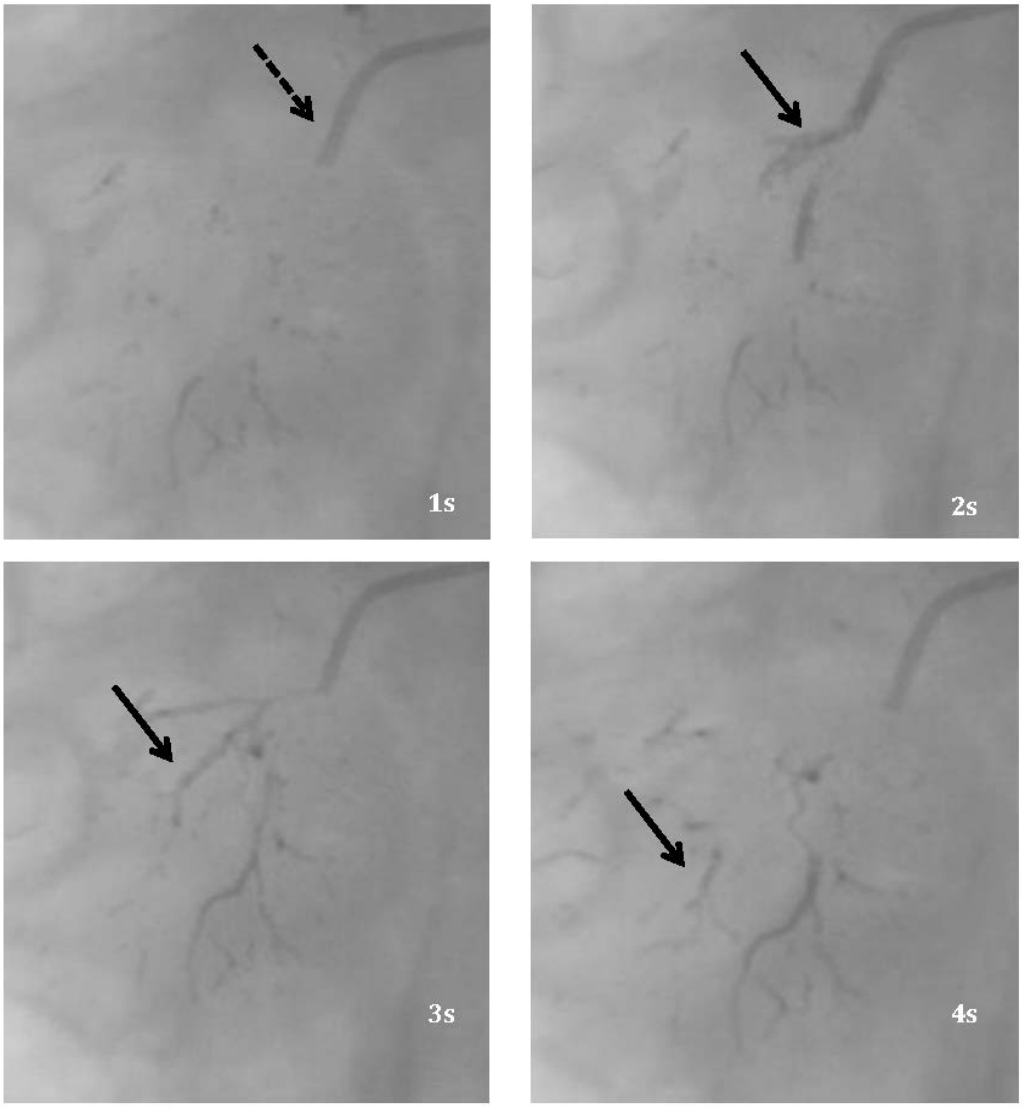


**Figure 1:** Injection of Zn–Si microspheres, demonstrating the temporal and spatial distribution for 300-500 $\mu$m Zn–Si microspheres.

rial occlusion; 1=reduction of parenchymal staining of the dependent territory; 2=reduction of the parenchymal staining and occlusion of the supplying arcuate artery; 3=reduction of parenchymal staining, occlusion of the supplying arcuate artery and occlusion of the feeding artery downstream of the catheter tip.

As an additional measure, blood samples (and animal weights) were collected by venipuncture for all animals in cohort II under anesthesia at Days 0, 1, 7, 14 and pre-euthanasia to enable standard clinical laboratory tests for haematology and clinical chemistry. Day 1 clinical laboratory data was used as an internal reference range to assess individual and group mean values. During the follow-up interval, animals were closely monitored for any occurrence of post-embolization syndrome (such as, malaise, fever, vomiting).

## 2.3 Gross Pathology, Diagnostic Imaging and Histology.

### 2.3.1 Gross Pathology and CT Evaluation.

For cohort I and II, animals were euthanized (while under anesthesia) the day of embolization and at 29 days post-embolization, respectively. Euthanasia was by lethal injection of saturated potassium chloride (KCl, rapid IV bolus). A standard postmortem procedure was performed with gross pathological examination. Animals in cohort I

were subjected to a full body CT scan (Siemens Somatom Sensation 16, Siemens Healthcare, Erlangen, Germany) to evaluate for possible imaging artifacts from the Zn–Si microspheres.

#### 2.3.2 High Resolution Radiographs and Micro-CT.

Whole fixed kidneys, embolized with Zn–Si microspheres (both cohorts) were analyzed using a Faxitron MX-20 radiography system (Faxitron X-ray Corp, Wheeling, IL) to identify the embolized arteries for histology processing. Subsequently, the embolized arteries were scanned using a Skyscan Micro CT scanner (Skyscan, Antwerp, Belgium). Transmission images were used to create a stack of 2D images using the Nrecon program (Skyscan, Kontich, Belgium) before a 3D model was created to visualize the respective embolized region.

#### 2.3.3 Histology.

Embolized renal arteries identified from the high resolution kidney radiographs were subsequently harvested, fixed and sectioned, prior to embedding in methyl methacrylate/N Butyl methacrylate resin (LabMAT, Québec, QC, Canada), Subsequent sections were ground into radial slides (approximately 50 $\mu$m) and stained with (a) Haemotoxylin and Eosin and (b) Verhoeff-Van Gieson (V-VG), per Araki *et al.* [20]. Observations were subjectively graded by an independent Study Pathologist (AccelLabs, Montral, QC, Canada), using the following scale as a guide:

- Minimal: observation is barely perceptible microscopically, and is not believed to have clinical significance.
- Mild: observation is visible but involves a minor proportion of the tissue, and the clinical consequences of the observation are most likely subclinical.
- Moderate: observation is clearly visible and involves a significant proportion of the tissue; it is likely to have some clinical manifestations, but which are generally expected to be minor.
- Marked: observation is clearly visible and involves a major proportion of the tissue; clinical manifestations are probable, and may be associated with significant tissue dysfunction or damage.

Finally, sections were examined using light microscopy (TMS-F, Nikon, Tokyo, Japan), with the microsphere diameter and inner diameter of the arteries where the microspheres lodged measured using quantitative morphometric computer-assisted methods via Image Pro Plus 6.1.0.346 software.

## 3 Results

Given its radiolucency, Embosphere® could not be directly imaged during RAE. By comparison, the delivery of Zn-Si microspheres provided for direct visualization *(in each particle size range)* within the renal vasculature under fluoroscopic imaging. Temporal and spatial distribution of Zn–Si microspheres is illustrated in Figure 1, such that at:

- 1s, catheter tip (dashed arrow), including previously injected Zn-Si microspheres seen in the distal renal artery branches, were visible under routine fluoroscopy.
- 2s, the Zn–Si microspheres were visible upon injection from the catheter tip (plain arrows).
- 3s, the Zn–Si microspheres had a spatial distribution, which could be visualized using standard fluoroscopy techniques.
- 4s, the final spatial distribution for the Zn–Si microspheres.

Prior to embolization, all embolization scores were graded a score of 0. Procedural success of the targeted arteries, with effective stasis and no flow beyond the embolized areas were observed for all animals. Immediately post-embolization, complete embolization effectiveness (3) was observed for all animals. Furthermore, no acute complications (perforation or rupture) were noted throughout any of the embolization procedures. Table 2 presents the change in embolization scores for experimental and control microsphere, recorded immediately post-embolization and 29 days post-embolization, for the latter the mean embolization scores for Zn–Si glass and Embosphere® decreased to 2.3 (extensive) and 1.5 (slight to extensive), respectively.

Cortical tissue reduction was confirmed on follow-up arteriograms for all animals in cohort II. Varying degrees of arterial recanalization (recanalization being the restoration of partial blood flow within the embolized artery) could be identified for Embosphere embolized arteries but no recanalization could be seen in Zn–Si embolized arteries. On microscopic evaluation, both materials appeared to exhibit varying degrees of recanalization, though based on the pilot study, it appeared that both materials are comparable with respect to recanalization and durability of oc-

**Table 2:** Embolization scores for each animal in cohort II.

| Cohort/Animal No. | Material | Embolization Score[1]/Anatomical Location[2] | |
|---|---|---|---|
| | | Immediately Post-embolization | 29 Days Post-embolization |
| **Cohort II/Ac-04** | Zn–Si glass | 3/Cr-LRA | 3/Cr-LRA |
| **Cohort II/Ac-05** | Embosphere® | 3/Ca-LRA | 1/Ca-LRA |
| **Cohort II/Ac-06** | Zn–Si glass | 3/Cr-RRA | 2/Cr-RRA |
| **Cohort II/Ac-07** | Embosphere® | 3/Cr-RRA | 2/Cr-RRA |
| **Cohort II/Ac-08** | Zn–Si glass | 3/Cr-LRA | 2/Cr-LRA |

[1]Where 0= No angiographically visible signs of arterial occlusion; 1=reduction of parenchymal staining of the dependent territory; 2=reduction of the parenchymal staining and occlusion of the supplying arcuate artery; 3=reduction of parenchymal staining, occlusion of the supplying arcuate artery and occlusion of the feeding artery downstream of the catheter tip.
[2] Where Cr=Cranial, Ca=Caudal, LRA=Light renal artery, RRA=Right renal artery.

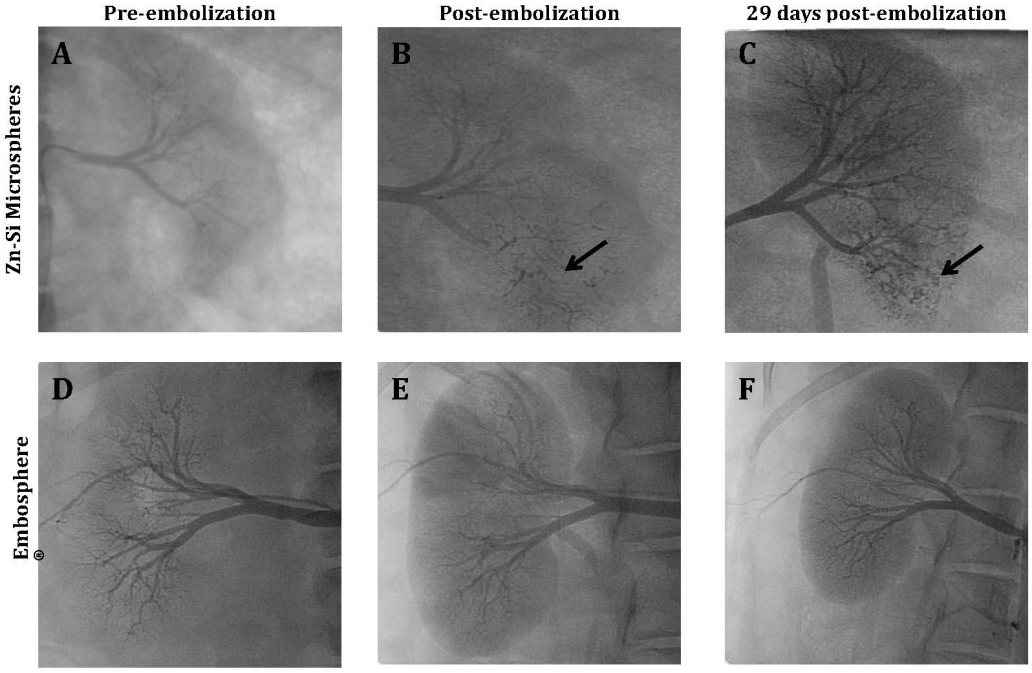


**Figure 2:** Selective renal arteriograms with 40-150 $\mu$m Zn–Si glass (Ac-01) versus 40-120 Embosphere® (Ac-04) microspheres: pre-embolization (A and D), immediately post-embolization (B and E) and 29 days post-embolization (C and F).

clusion. Figure 2 provides substantiating fluoroscopic data to support the embolization scores provided in Table 2.

Specific to cohort II, all animals remained in good health throughout the entire follow-up period. Animals gained between 0.7-3.0 kg during the study (1.83 kg for Zn–Si glass versus 2.7 kg Embosphere® treated animals, respectively). Blood samples collected at 0, 1, 7, 14 and 29 days (pre-euthanasia) and analyzed using standard clinical laboratory tests showed minor fluctuations in white blood cell count, total proteins, aspartate amino-transferase and creatinine kinase values were noted in all animals (full hematology analysis is provided as supplemental information for completeness). Slightly elevated fibrinogen levels were noted in all animals, but resolved

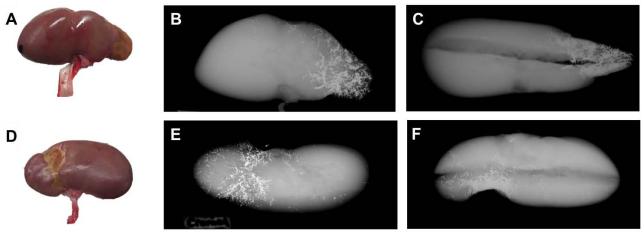


**Figure 3:** Representative images of gross pathology and high-resolution kidney radiographs for cohort II. Harvested kidneys (A and D) and images of the anterior (B and E) and lateral (C and F) view of the left kidney for animals Ac-04 (A to C) and Ac-06 (D to F), embolized with 40-150 $\mu$m Zn–Si glass, clearly demonstrate clear depressions of the embolized regions for histology processing and evaluationc.


**Figure 4:** Whole animal CT (left and right kidney coronal plane, Ac-02 (B) and Ac-03 (A)) and (left and right kidney coronal and axial planes, Ac-03 (C)) and Micro-CT (Ac-01, D) scans.

within the first week. These short-lived changes were considered secondary to the renal embolization and part of the normal physiological response to the biomaterials and anesthetic.

Kidneys were harvested and examined ex-vivo immediately post mortem. Macroscopic abnormalities and shrinkage of the embolized region were seen for all embolized kidneys (Figure 3). The embolization region could clearly be distinguished from the contralateral untreated kidney (or the embolized targeted kidney area) 29 days post-embolization (Figure 3A and 3D). As such, firm, generally depressed areas of varying colours and sizes on the renal surface and extending into the parenchyma of the embolized kidneys were noted. Lateral and anterior views of the kidney displayed clear spatial distribution of the microspheres when visualized under high-resolution radiography (Figure 3B, 3C, 3E and 3F). This imaging modality allowed mapping of the microsphere localization throughout the kidney, corroborating the earlier macroscopic findings while identifying regions for histological processing.

Figure 4 is a whole body CT scan (Ac-02 and Ac-03) with micro-CT reconstruction (Ac-01) and illustrates the high visibility and potential for assessment of spatial distribution of the Zn–Si microspheres within the renal vasculature. Conversely, the spatial distribution of the conventional embolic agent (caudal pole, right hand side) is impossible to assess.

Zn–Si microspheres did not uptake the stain and appeared smooth and transparent versus Embosphere® which displayed a fuchsia colour upon staining. Minimal to mild acute inflammation was seen in the adventitia of 25% of Zn–Si glass embolized artery/branch sections (small black arrows, Figure 5B). For Embosphere® treated animals, minimal infiltration of mononuclear cells were observed in 70% (against 57% for Zn–Si microspheres) in the peri-arteriolar tissue. Connective tissue was visible between adjacent microspheres in an occluded vessel for both groups (long black arrow, Figure 5A and 5B). Histopathology evaluation did not indicate necrosis or other microscopic abnormality in the renal artery or renal parenchyma arterioles. The inflammatory reaction observed between both microspheres and the surrounding tissues were composed of mononuclear cells (lymphocytes, polymorphonuclear and plasma cells). Overall, Embosphere® were observed in 90% of the kidney sections, while Zn–Si microspheres were observed in 100% of the analyzed sections partially to completely occluding arterioles of various size.

For all embolized kidneys in cohort II, both materials were shown to occlude arterioles in all kidney sections (Figure 5) analyzed. Zn-Si microspheres did not deform as confirmed by micro CT versus Embosphere®. Connective tissue was visible between Embosphere® in one occluded vessel. 29 days post-embolization, all animals displayed signs of chronic inflammation and mononuclear cell infiltration (small black arrows, Figure 5B and 5E); multifocal disruption of the internal elastic lamina (IEL, Figure 5C) sometimes associated with mineralization of the ves-

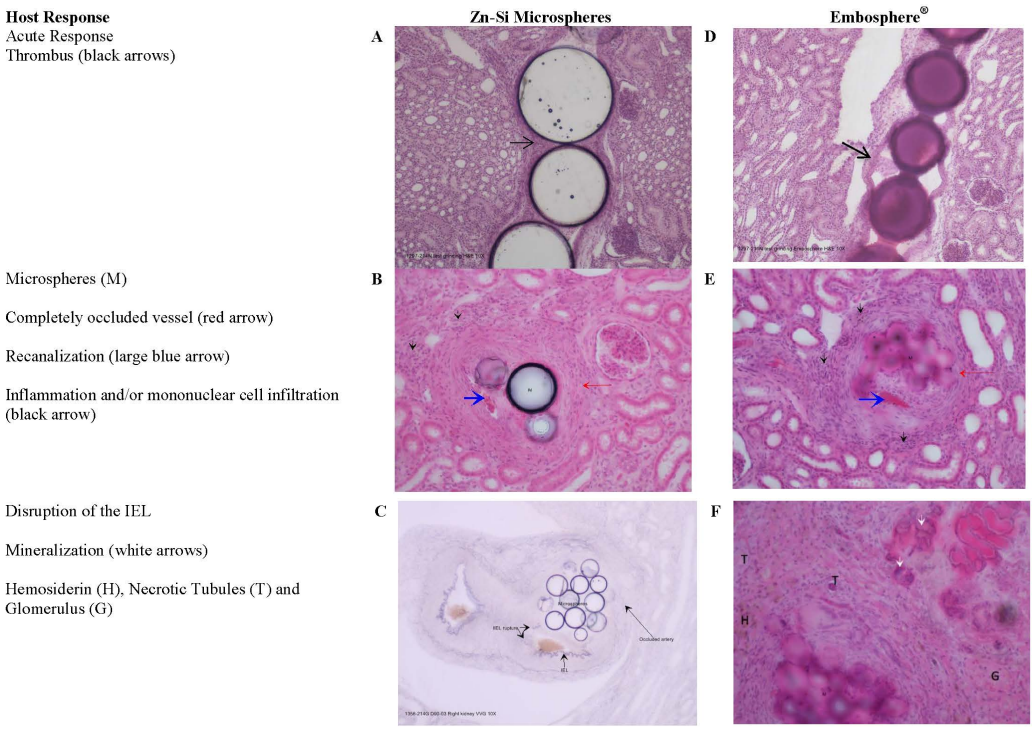


**Figure 5:** Acute (magnification 10×) and subchronic (magnification 10× (C) and 20× (B, E and F) histopathologic evaluation of swine RAE with Zn–Si glass and Embosphere® microspheres.

sel wall (white arrows, Figure 5F) and vessel recanalization (see Figure 5B and 5E, blue arrows). Moderate kidney infarction, described as necrotic tubules and glomerulus (annotated T and G respectively in image F, Figure 5), and hemosiderin (annotated H in Figure 5F) was also observed. Additionally, Embosphere® displayed occasional disruption of the external elastic laminated (EEL).

## 4 Discussion

The swine RAE model was chosen for this study as significant similarities are known to exist between the swine and human renal vasculature [4, 5, 7, 8, 21–25]. Cohort I enabled the evaluation of real-time spatial and temporal distribution (Figure 1), ease of deliverability, embolization effectiveness (Table 2) and acute local host response for (a) 40-150 $\mu$m, (b) 150-300 $\mu$m and (c) 300-500 $\mu$m Zn–Si microspheres versus an equivalent control (Figure 5). Cohort II enabled sub-chronic evaluations (29 days) of 40-150 $\mu$m Zn–Si microspheres (versus an equivalent control). The 40-150 $\mu$m microspheres were selected for subchronic evaluations as they represent the worst-case scenario in terms of highest surface area to volume ratio, they are also the most challenging to image, and furthermore, have the greatest potential to migrate to distal locations [21, 24]. The use of Zn–Si microspheres provided direct intraprocedural feedback using standard diagnostic imaging techniques for all particle size ranges examined. It is clear from the data presented in this work, that the clinical deployment of imageable beads, provides a valuable tool to interventional radiologists to formulate and standardize TAE procedures. In a clinical setting, these microspheres permit the definition of spatial distribution (Figure 4) in a target tissue, consequently permitting the optimization, personalization and improvement of TAE techniques. It was noted that the Zn–Si microspheres appeared to offer more predictable occlusion than the control during these procedures, a feature which may be attributable to the non-compressible nature of the glass microspheres versus the high compressibility of the control article. Further levels of occlusion studies are required to confirm this hypothesis. However, given their non-compressible nature, an upper limit of compatible particle size distributions with conventional micro-catheters (where internal diameters are c. 700 $\mu$m) is noted.

For animals in cohort II, no acute complications were reported (*i.e.* perforation or rupture). All animals survived to their scheduled euthanasia after embolization (with

no signs of bacterial colonization). The minor fluctuations observed (see supplemental information/section 3) during clinical pathology evaluations were attributed to stress as opposed to being a direct effect of the treatment. Upon macroscopic examination, clear depressions of the embolized area were noted as expected (Figure 3A). Furthermore, the loco-regional distribution of the Zn-Si microspheres were clearly visible on high-resolution radiographs and CT (Figure 3 and 4), without contiguous imaging artifacts; the latter point being important as imaging artifacts can complicate follow-up diagnostic imaging.

Diameters of the occluded renal parenchyma arterioles appeared to be larger for the Zn–Si microspheres versus Embosphere®. Standard histology processing however, is known to affect vessel and material dimensions (leading to a reduction of biological tissues up to 10%) [24]. For cohort I, no necrosis or other abnormalities were revealed. Incomplete endothelial coverage (yellow arrows, Figure 5) and minimal acute tubular necrosis were noted with both materials, and were interpreted by the Study Pathologist as being secondary to the procedure. Direct contact of the vessel wall with both materials appeared to show mechanical occlusion (Figure 5), with thrombus formation filling gaps between adjacent microspheres and the vascular walls (black arrows, Figure 5A and 5D). Mononuclear cells (70% for Embosphere® versus 57% for Zn-Si microspheres) were observed for both materials. However, no significant differences were noted between the materials in terms of marked inflammatory reactions. It appeared that both materials were comparable with respect to recanalization and durability of occlusion (see Figure 5A and 5B, blue arrows) (proposed mechanisms of recanalization comprise angiogenesis, capillary regrowth, thrombus resorption or re-distribution of the microspheres [26, 27]).

In cohort II, no degradation of material was observed for either material over the course of the 29 day implantation period. Microscopic observations showed kidney infarction, partial to complete occluded arterioles, mononuclear cell infiltration (small black arrows in Figure 5B and 5E), hemosiderin (annotated H, Figure 5F), necrotic tubules and glomerulus (annotated T and G respectively, Figure 5F) for both materials. The V-VG stain permits the staining of elastic fibers which become exposed due to disruptions in the elastic laminae of arteries. Figure 5(C) illustrates the observed V-VG staining for Zn–Si microspheres and shows minor disruptions to the elastic laminae in a fashion consistent with other embolization products [28–30]. In addition to disruption of the elastic laminae, mineralization of the vessel wall was also observed for Embosphere® (white arrows, Figure 5F), attributed to the material triggering cell devitalization, preventing phosphorus membranes to properly function, and ultimately resulting in the formation of calcium phosphate crystals [31].

# 5 Conclusion

The use of Zn–Si microspheres, provided direct intraprocedural feedback using standard diagnostic imaging techniques for all particle size ranges examined. It is clear from the data presented in this work, that the clinical deployment of imageable beads, provides a valuable tool to interventional radiologists to formulate and standardize TAE procedures. In a clinical setting, these microspheres permit the definition of spatial distribution in a target tissue, consequently permitting the optimization, personalization and improvement of TAE techniques. In this swine RAE model, histopathology evaluation showed vessel occlusion with infarction of the embolized kidney pole without additional adverse tissue reaction. The histopathological responses were relatively similar between the Zn-Si glass and Embosphere® materials, demonstrating overall safety and efficacy of Zn-Si microspheres in a sub-chronic large animal study. Further analysis need to be performed to assess device migration as no histology evaluation of the animal external organs was carried out during the course of this study.

**Acknowledgement:** The authors wish to acknowledge the technical services of AccelLabs (Montreal, QC, Canada) for participating in this research study.

# References

[1] Baino F., Novajra G., Miguez-Pacheo V., Boccaccini A.R., Vitale-Brovarone C., Bioactive Glasses: Special Applications outside the Skeletal System, J. Non. Cryst. Sol. 2015, XXX, XXX-XXX

[2] Laurent A., Microspheres and Nonspherical Particles for Embolization, Techn. Vasc. and Inter. Radiol. 2007, 10, 248-256

[3] Ryu R., Uterine Artery Embolization: Current Implications of Embolic Agent Choice, J. Vasc. Inter. Radiol. 2005, 16, 1419-1422

[4] Sharma K.V., Dreher M.R., Tang Y., Pritchard W.F., Chiesa O.A., Karanian J., *et al.*, Development of "Imageable" Beads for Transcatheter Embolotherapy, J. Vasc. Interv. Radiol. 2010, 21, 865–876

[5] Dreher M.R., Sharma K.V., Woods D.L., Reddy G., Tang Y., Pritchard W.F., *et al.*, Radiopaque Drug-Eluting Beads for Transcatheter Embolotherapy: Experimental Study of Drug Penetration and Coverage in Swine, J. Vasc. Interv. Radiol. 2012, 23, 257–264

[6] Lu X.J., Zhang Y., Cui D.C., Meng W.J., Du L.R., Guan H.T., *et al.*, Research of Novel Biocompatible Radiopaque Microcapsules for Arterial Embolization, Int. J. Pharm. 2013, 452, 211-219

[7] Stampfl S., Stampfl U., Bellemann N., Sommer C.M., Thierjung H., Radeleff B., *et al.*, Biocompatibility and Recanalization Characteristics of Hydrogel Microspheres with Polyzene-F as Polymer Coating, Cardiovasc. Interv. Radiol. 2008, 31, 799–806

[8] Siskin G.P., Dowling K., Virmani R., Jones R., Todd D., Pathologic Evaluation of a Spherical Polyvinyl Alcohol Embolic Agent in a Porcine Renal Model, J. Vasc. Interv. Radiol. 2003, 14, 89–98

[9] Spies J.B. Uterine Artery Embolization for Fibroids: Understanding the Technical Causes of Failure, J. Vasc. Interv. Radiol. 2003, 14, 11–14

[10] Lopera G., Embolization in Trauma: Principles and Techniques, Semin. Interv. Radiol. 2010, 27, 14–28

[11] Kehoe S., Tonkopi E., Abraham R., Boyd D., Predicting the Thermal Responses and Radiopacity of Multicomponent Zinc–Silicate Bioglasses: A focus on ZnO, $La_2O_3$, $SiO_2$ and $TiO_2$, J. Non. Cryst. Sol. 2012, 358, 3388–3395

[12] Kehoe S., Kilcup N., Boyd D., Evaluation of Cytotoxicity for Novel Composite Embolic Microspheres: Material Optimization by Response Surface Methodology, Mat. Lett. 2012, 86, 13–17

[13] Kehoe S., Abraham R., Tonkopi E., Boyd D., Novel Radiopaque Embolic Agent for Uterine Fibroid Embolization: Determination of Radiopacity and Biological Evaluation; Cytocompatibility, Intracutaneous Reactivity and Local Effects after Implantation, J. Vasc. Interv. Radiol. 2011, 23, S33

[14] Kehoe S., Langman M., Werner-Zwanziger U., Abraham R.J., Boyd D., Mixture Designs to assess Composition-Structure-Property Relationships in $SiO_2$–CaO–ZnO–$La_2O_3$–$TiO_2$–MgO–SrO–$Na_2O$ Glasses: Potential Materials for Embolization, J. Biomater. App. 2013, 28, 416–433

[15] Kehoe S., Tremblay M.T., Coughlan A., Towler M.R., Rainey J.K., Abraham R.J., Boyd D., Preliminary Investigation of the Dissolution Behaviour, Cytocompatibility, Effects of Fibrinogen Conformation and Platelet Adhesion for Radiopaque Embolic Particles, J. Funct. Biomater. 2013, 4, 89–113

[16] Kehoe S. Looney M., Kilcup N., Tonkopi E., Daly C., Abraham R.J., Boyd D., Effects of $\gamma$-Irradiation and Accelerated Aging on Composition-Structure–Property Relationships for Radiopaque Embolic Microspheres, J. Non. Crystal. Sol. 2014, 402, 84–90

[17] Hasan M., Kehoe S., Boyd D., Temporal analysis of dissolution by-products and genotoxic potential of spherical zinc–silicate bioglass: "Imageable beads" for transarterial embolization, J. Biomater. App. 2014, 29, 566–581

[18] Pelage J.P., Polyvinyl Alcohol Particles versus Tris-acryl Gelatin Microspheres for Uterine Artery Embolization for Leiomyomas, J. Vasc. Interv. Radiol. 2004, 15, 789–791

[19] Stampfl S., Stampfl U., Rehnitz C., Schnabel Ph., Satzl S., Christoph P., *et al.*, Experimental Evaluation of Early and Long-Term Effects of Microparticle Embolization in Two Different Minipig Models, Part I: Kidney, Cardiovasc. Interv. Radiol. 2007, 30, 257–267

[20] Araki N., Nagata Y., Fujiwara K., Aoki T., Mitsumori M., Kimura H., *et al.*, Evaluation of Glass Microspheres for Intra-arterial Radiotherapy in Animal Kidneys, Int. J. Radiat. Oncol. Biol. Phys. 2001, 49, 459–463

[21] Stampfl S., Bellemann N., Stampfl U., Radeleff B., Lopez-Benitez R., Sommer C.M., *et al.*, Inflammation and Recanalization of Four Different Spherical Embolization Agents in the Porcine Kidney Model, J. Vasc. Interv. Radiol. 2008, 19, 577–586

[22] Andrews R.T., Binkert C.A., Relative Rates of Blood Flow Reduction during Transcatheter Arterial Embolization with Tris-acryl Gelatin Microspheres or Polyvinyl Alcohol: Quantitative Comparison in a Swine Model, J. Vasc. Interv. Radiol. 2003, 14, 1311–1316

[23] Bilbao J.I., de Luis E., García de Jalón J.A., de Martino A., Lozano M.D., de la Cuesta A.M., *et al.*, Comparative Study of Four Different Spherical Embolic Particles in an Animal Model: A Morphologic and Histologic Evaluation, J. Vasc. Interv. Radiol. 2008, 19, 1625–1638

[24] Stampfl S., Bellemann N., Stampfl U., Sommer C.M., Thierjung H., Lopez-Benitez R., Arterial Distribution Characteristics of Embozene Particles and Comparison with other Spherical Embolic Agents in the Porcine Acute Embolization Model, J. Vasc. Interv. Radiol. 2009, 20, 1597–1607

[25] Swindle M.M., Makin A., Herron A.J., Clubb Jr. F.J., Frazier K.S., Swine as Models in Biomedical Research and Toxicology Testing, Veter. Pathol. 2012, 49, 344–356

[26] Siskin G.P., Englander M., Stainken B.F., Ahn J., Dowling K., Dolen E.G., Embolic Agents used for Uterine Fibroid Embolization, 2000, AJNR, 175, 767–773

[27] Laurent A., Wassef M., Namur J., Martal J., Labarre D., Pelage J.P., 2009, Recanalization and Particle Exclusion after Embolization of Uterine Arteries in Sheep: A Long-Term Study, Fertil. Steril. 2009, 91, 884–892

[28] Arakawa H., Murayama Y., Davis C.R., Howard D.L., Baumgardnera W.L., Marks M.P., Do H.M., Endovascular Embolization of the Swine Rete Mirabile with Eudragit-E 100 Polymer, Amer. J. Neuroradiol. 2007, 28, 1191–1196

[29] Germano I.M., Davis R.L., Wilson C.B., Hieshima G.B., Histopathological Follow-up Study of 66 Cerebral Arteriovenous Malformations after Therapeutic Embolization with Polyvinyl Alcohol, J. Neurosurg. 1992, 76, 607–614

[30] Davidson G.S., Terbrugge K.G., Histologic Long-Term Follow-up after Embolization with Polyvinyl Alcohol Particles, Amer. J. Neuroradiol. 1995, 16, 843–846

[31] Schoen F.J., Levy R.J., Calcification of Tissue Heart Valve Substitutes: Progress toward Understanding and Prevention, Ann. Thorac. Surg. 2005, 79, 1072–1080